Please cite this article in press as: Bernasconi et al., Role of the SEL1L:LC3-I Complex as an ERAD Tuning Receptor in the Mammalian ER, Molecular Cell (2012), doi:10.1016/j.molcel.2012.04.017

Molecular Cell
Article

Role of the SEL1L:LC3-I Complex as an ERAD Tuning Receptor in the Mammalian ER

Riccardo Bernasconi,[1] Carmela Galli,[1] Julia Noack,[1] Siro Bianchi,[1] Cornelis A.M. de Haan,[2] Fulvio Reggiori,[3] and Maurizio Molinari[1,4,*]
[1]Institute for Research in Biomedicine, CH-6500 Bellinzona, Switzerland
[2]Virology Division, Department of Infectious Diseases and Immunology, Faculty of Veterinary Medicine, Utrecht University, The Netherlands
[3]Department of Cell Biology, University Medical Center Utrecht, The Netherlands
[4]École Polytechnique Fédérale de Lausanne, School of Life Sciences, CH-1015 Lausanne, Switzerland
*Correspondence: maurizio.molinari@irb.usi.ch
DOI 10.1016/j.molcel.2012.04.017

SUMMARY

Several regulators of endoplasmic reticulum (ER)-associated degradation (ERAD) have a shorter half-life compared to conventional ER chaperones. At steady state, they are selectively removed from the ER by poorly defined events collectively referred to as ERAD tuning. Here we identify the complex comprising the type-I transmembrane protein SEL1L and the cytosolic protein LC3-I as an ERAD tuning receptor regulating the COPII-independent, vesicle-mediated removal of the lumenal ERAD regulators EDEM1 and OS-9 from the ER. Expression of folding-defective polypeptides enhances the lumenal content of EDEM1 and OS-9 by inhibiting their SEL1L:LC3-I-mediated segregation. This raises ERAD activity in the absence of UPR-induction. The mouse hepatitis virus (MHV) subverts ERAD tuning for replication. Consistently, SEL1L or LC3 silencing impair the MHV life cycle. Collectively, our data provide new molecular information about the ERAD tuning mechanisms that regulate ERAD in mammalian cells at the post translational level and how these mechanisms are hijacked by a pathogen.

INTRODUCTION

Most nascent polypeptide chains entering the ER are covalently modified with preassembled oligosaccharides composed of 2 N-acetylglucosamine, 9 mannose and 3 glucose residues (Figure S1A). Failure to attain the native structure is signaled by the progressive removal of 2 to 4 terminal mannose residues. Dedicated ERAD lectins eventually deliver partially demannosylated, terminally misfolded proteins to dislocons, i.e., sites of protein retrotranslocation across the ER membrane built around membrane-embedded E3 ubiquitin ligases (Hebert et al., 2010; Smith et al., 2011; Vembar and Brodsky, 2008). In the "mannose timer model" of protein quality control (Helenius, 1994), the ER mannosidase I (ERManI), EDEM proteins, OS-9 and XTP3-B variants use their mannosidase-like (ML) or their mannose 6-phosphate receptor homology (MRH) domains to generate and/or to recognize the oligosaccharide-based signal on misfolded polypeptides to be channeled into one of the many eukaryotic ERAD pathways (Aebi et al., 2010; Lederkremer, 2009). Recently, it has been reported that EDEM1, OS-9 and XTP3-B (and their yeast orthologs; Hanna et al. [2012]) may use their ML or MRH domains to associate with oligosaccharides displayed by the type I membrane protein SEL1L, a component of the dislocation machinery containing the E3 ubiquitin ligase HRD1 (Christianson et al., 2012; Christianson et al., 2008; Cormier et al., 2009; Satoh et al., 2010). This led to challenge the "mannose timer model" of protein quality control and to propose an alternative "docking model" of protein quality control in which oligosaccharides may serve as docking sites for EDEM1 and OS-9 at the SEL1L/HRD1 dislocon, rather than as signal tagging misfolded polypeptides for destruction (Aebi et al., 2010; Tamura et al., 2010). In this work, we have evaluated the consequences and the biological relevance of the oligosaccharide-based association between EDEM1 or OS-9 and SEL1L.

The ERAD regulators EDEM1 and OS-9 have shorter half-lives compared to conventional ER chaperones and enzymes (Figure S1B). At steady state, they are selectively released from the ER by a COPII-independent vesicular pathway to be eventually degraded by endosomal/lysosomal proteases (Calì et al., 2008; Le Fourn et al., 2009; Reggiori et al., 2010; Zuber et al., 2007). This is a facet of series of poorly defined events collectively named ERAD tuning that sets steady state ERAD activity at levels that do not compromise protein biogenesis by insuring a constitutive and selective clearance of ERAD factors from the ER (Bernasconi and Molinari, 2011). The presence of the ubiquitin-like protein LC3-I noncovalently associated at the cytosolic surface, distinguishes the ER-derived, ERAD tuning vesicles containing EDEM1 and OS-9 (named EDEMosomes in Calì et al., [2008] and Reggiori et al., [2010]) from autophagosomes where LC3 is covalently bound to the membrane lipid phosphatidylethanolamine and is therefore named LC3-II (Kabeya et al., 2000). Conventional ER markers are excluded from ERAD tuning vesicles (Calì et al., 2008; Zuber et al., 2007) and from similar EDEM1/OS-9/LC3-I-containing vesicles co-opted for replication by the mouse hepatitis virus (MHV), a prototype coronavirus (CoV) (de Haan et al., 2010; Reggiori et al., 2010). This implies a receptor-mediated selection of EDEM1 and OS-9 in the ER lumen for segregation in these LC3-I$^+$ structures (Bernasconi and Molinari, 2011).

Please cite this article in press as: Bernasconi et al., Role of the SEL1L:LC3-I Complex as an ERAD Tuning Receptor in the Mammalian ER, Molecular Cell (2012), doi:10.1016/j.molcel.2012.04.017

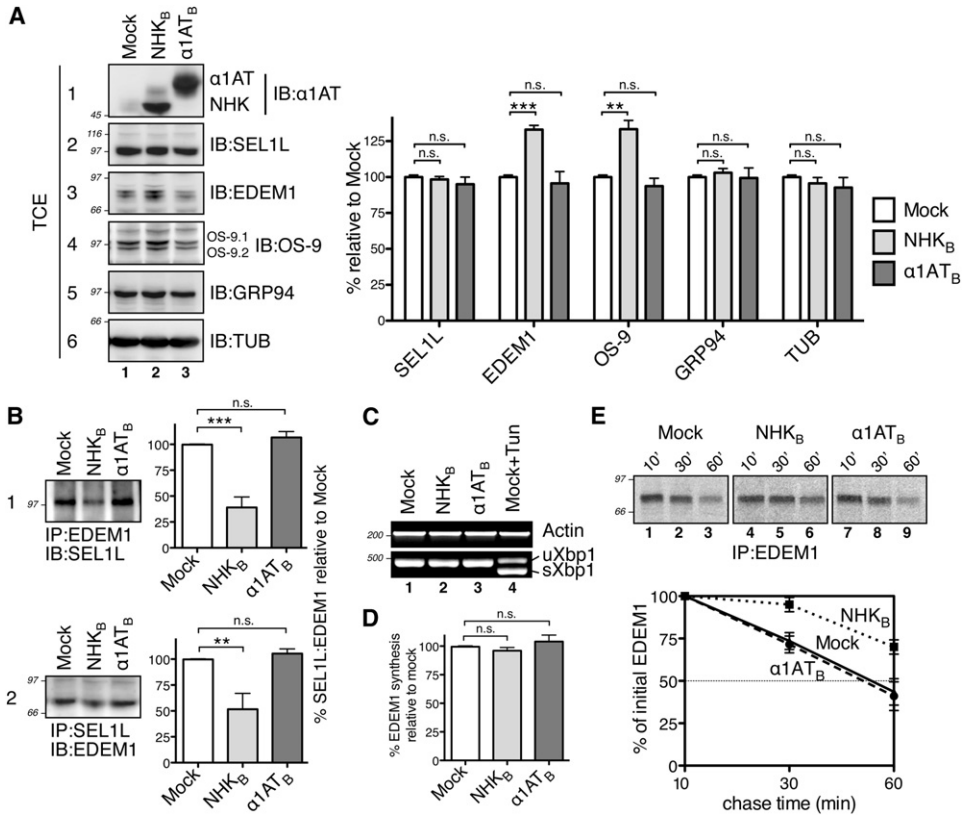

Figure 1. Endogenous Complexes between EDEM1 and SEL1L

(A) Levels of NHK_B, $\alpha1AT_B$, SEL1L, EDEM1, OS-9, GRP94 and Tubulin in HEK293 with stable expression of empty plasmid (Mock, lane 1), NHK_B (lane 2) or $\alpha1AT_B$ (lane 3) are monitored by western blots in panels 1–6, respectively and quantified.

(B) Endogenous SEL1L that coprecipitates with endogenous EDEM1 (panel 1, with quantifications) and endogenous EDEM1 in endogenous SEL1L immunoisolates (panel 2, with quantifications).

(C) Amplification by RT-PCR of unspliced (u) and spliced (s) Xbp1 transcripts (Mock+Tun, positive control of ER stress).

(D) Quantification of ^{35}S-met/cys incorporation in endogenous EDEM1 immunoisolated from cell lysates.

(E) Turnover of endogenous EDEM1 in the stable cell lines. Error bars: standard deviations from the mean of three replicates.

Here we identify SEL1L as the elusive ERAD tuning receptor that selectively captures EDEM1 and OS-9 in the ER lumen, thereby insuring their constitutive clearance from the ER at steady state. The proline-rich, cytosolic tail of SEL1L binds LC3-I and is required and sufficient for segregation of the receptor and its cargo into the ERAD tuning vesicles. EDEM1 and OS-9 use their ML and MRH domains to bind misfolded polypeptides or SEL1L oligosaccharides (Christianson et al., 2012; Christianson et al., 2008; Cormier et al., 2009; Hanna et al., 2012; Satoh et al., 2010). By engaging EDEM1 and OS-9, and by stabilizing SEL1L in the HRD1 dislocon, folding-defective polypeptides compete with the formation of the ERAD tuning complexes containing EDEM1, OS-9, SEL1L and LC3-I. This inhibits the constitutive removal of EDEM1 and OS-9 from the ER thereby enhancing lumenal ERAD activity in the absence of unfolded protein response (UPR) induction. Consistent with data showing that the ER-derived EDEM1/OS-9/LC3-I-containing vesicles are co-opted by CoV for replication (de Haan et al., 2010; Reggiori et al., 2010), we report that the newly identified ERAD tuning receptor component SEL1L also localizes in these vesicles in MHV-infected cells and that silencing of either SEL1L or of LC3 inhibits MHV replication.

RESULTS

Expression of Folding-Defective Polypeptides Inhibits the Formation of Endogenous EDEM1:SEL1L Complexes

Ectopically expressed EDEM1 and OS-9 may use their ML or their MRH domains to associate with SEL1L oligosaccharides (Christianson et al., 2008; Cormier et al., 2009; Hanna et al., 2012; Satoh et al., 2010). We first verified whether these associations also occur between the endogenous proteins and whether the expression of folding-defective or folding-competent polypeptides in the ER lumen affects the intracellular level of EDEM1:SEL1L complexes. To this end, we generated three stable HEK293 lines that do not express any ectopic protein in the ER (Figures 1A and 1B, Mock), that express the folding-defective NHK_B (a membrane-bound variant of the ERAD substrate NHK) or the folding-competent, membrane-bound

secretory protein α1AT$_B$ (Figures 1A and 1B, lanes 2 and 3, respectively). The immunoisolation of endogenous EDEM1 from the detergent lysates of Mock cells and the analysis of the immunoprecipitates by western blot confirmed the coimmunoisolation of endogenous SEL1L (Figure 1B, panel 1, lane 1). Consistently, the immunoisolation of endogenous SEL1L combined with the characterization of the immunoprecipitates by western blot revealed the presence of endogenous EDEM1 in the immunoprecipitates (Figure 1B, panel 2, lane 1). This proved the presence of complexes between endogenous EDEM1 and SEL1L at steady state in cultured HEK293 cells. Expression of the folding-defective NHK$_B$ (Figure 1B, panels 1 and 2, lane 2), but not expression of the folding-competent α1AT$_B$ (lane 3), substantially reduced the abundance of these complexes (Figure S2A confirms these data with ectopically expressed (r) EDEM1). Interestingly, cells expressing the ERAD substrate, but not cells expressing the folding-competent protein, contained higher levels of SEL1L:HRD1 complexes (Figure S2B, panel 4), which play a crucial role in NHK disposal (Bernasconi et al., 2010). Thus, ER loading with misfolded polypeptides inhibits formation of EDEM1:SEL1L complexes, while favoring SEL1L association with the HRD1-containing dislocon.

Expression of Folding-Defective Polypeptides Enhances the Intracellular Content of EDEM1 and OS-9 in the Absence of UPR Induction

The analysis of our cell lines revealed that cells expressing NHK$_B$ contain higher levels of EDEM1 (Figure 1A, panel 3, lane 2) and OS-9 (panel 4, lane 2) than control cells (lane 1) or cells expressing α1AT$_B$ (lane 3 and quantifications). The rise in the EDEM1 and OS-9 levels in cells expressing the folding-defective NHK$_B$ did not result from UPR induction. In fact, the transcripts for the ER stress-induced spliced version of Xbp1 (sXbp1) were absent in all cell lines (Figure 1C, lanes 1–3; cell treatment with tunicamycin is shown as a positive control for ER stress, lane 4). Likewise, the intracellular level of the stress-inducible protein GRP94 (Figure 1A, panel 5 and quantification) and the synthesis of endogenous EDEM1 as determined by a quantitative analysis of [^{35}S]-Met/Cys incorporation in EDEM1 nascent chains remained unaffected upon NHK$_B$ expression (Figure 1D). Rather, our analysis revealed that the increased level of endogenous EDEM1 in cells expressing NHK$_B$ should be ascribed to its slower turnover (Figure 1E, lanes 4–6) compared to control cells (lanes 1–3) and to cells expressing the α1AT$_B$ (lanes 7–9, quantifications). Thus, the lumenal expression of the folding-defective NHK$_B$ reduces the amount of EDEM1:SEL1L complexes (Figures 1B and S2A) and delays the turnover of endogenous EDEM1 (Figure 1E) thereby raising its intracellular content in the absence of UPR induction (Figures 1A, 1C, and 1D). Based on these data, we hypothesized that formation of EDEM1:SEL1L complexes might regulate EDEM1 turnover and that SEL1L might be the elusive ERAD tuning receptor insuring the constitutive, vesicular-mediated removal of EDEM1 and OS-9 from the ER lumen (Calì et al., 2008; Reggiori et al., 2010).

SEL1L Enters EDEM1-Containing Vesicles

Electron microscopy studies revealed that EDEM1 is released from the ER in vesicles lacking a COPII coat (Zuber et al., 2007). Characterization of these vesicles by immunofluorescence and their separation in isopycnic density gradients showed that they also contain OS-9 and display the ubiquitin-like protein LC3-I noncovalently associated at the surface (Calì et al., 2008; Reggiori et al., 2010). Abundant ER proteins such as CNX, GRP94 and PDI are excluded from the EDEM1-containing ERAD tuning vesicles and from the EDEM1- and viral RNA-containing vesicles found in MHV infected cells (de Haan et al., 2010; Reggiori et al., 2010). This implies the intervention of an ERAD tuning receptor that selects the cargo proteins to be cleared from the ER. A role of SEL1L as ERAD tuning receptor would imply a dual localization of endogenous SEL1L in the ER and in the ERAD tuning vesicles. To assess this, EDEM1-containing vesicles were stabilized by exposing cultured HeLa cells to the lysosomotropic drug chloroquine (CQ), which prevents their fusion with LAMP1-containing degradative organelles (Calì et al., 2008; Reggiori et al., 2010). The immunofluorescence analysis of the cells confirmed the ER localization of SEL1L (Figure 2A) (Mueller et al., 2006) and showed that a fraction of endogenous SEL1L was in discrete vesicles lacking conventional ER protein markers (arrowheads in Figure 2A), a COPII coat (Figure S3A) and the autophagosome marker GFP-LC3 (Figure S3B), but containing EDEM1 (arrowheads in Figure 2B) and LC3 (Figures 2C–2D). The dual localization of SEL1L in the ER and in the ERAD tuning vesicles was confirmed upon their separation in isopycnic density gradients (Figure 2E) (Calì et al., 2008). These data would be consistent with the engagement of SEL1L as an ERAD tuning receptor that regulates the clearance of select ERAD factors from the ER lumen.

LC3-I Binds the Cytosolic Tail of SEL1L

The colocalization of SEL1L and LC3 in the ERAD tuning vesicles (Figures 2C–2E), prompted us to test whether LC3-I directly binds to the cytosolic tail of SEL1L. To verify this, HeLa cells were mock-transfected (Figure 3A, lane 1) or were transfected with a plasmid for expression of HA-tagged LC3$_{G120R}$ (LC3-I-HA, Figure 3A, lane 2). The G120R mutation prevents the covalent association with phosphatidyl-ethanolamine. LC3$_{G120R}$ is therefore inactive in autophagy and it does not label autophagosomes. In contrast, it associates with the membranes of the EDEM1-containing vesicles, both in noninfected and in MHV-infected cells (Reggiori et al., 2010). SEL1L (Figure 3A, panels 1 and 2) or CNX (Figure 3A, panels 3 and 4), an ER-resident type-I transmembrane protein with a cytosolic tail used here as a specificity control, were immunoisolated from cell lysates. The immunocomplexes were separated in SDS-PAGE and analyzed by western blot with an anti-LC3 antibody. LC3-I was found in immunocomplexes containing endogenous SEL1L (Figure 3A, panel 2, lane 2), but not in those containing CNX (panel 4, lane 2) thus showing the specificity of the association between LC3-I and SEL1L. To further confirm the specificity of this interaction and the direct involvement of the cytosolic tail of SEL1L in LC3-I binding, SEL1L, SEL1L$_{CNX}$ (SEL1L with the transmembrane and cytosolic tail of CNX), CNX and CNX$_{SEL1L}$ (CNX with the transmembrane and cytosolic tail of SEL1L) were ectopically expressed in HeLa cells to serve as baits for LC3-I-HA. Analysis of the immunocomplexes as described above confirmed the

Please cite this article in press as: Bernasconi et al., Role of the SEL1L:LC3-I Complex as an ERAD Tuning Receptor in the Mammalian ER, Molecular Cell (2012), doi:10.1016/j.molcel.2012.04.017

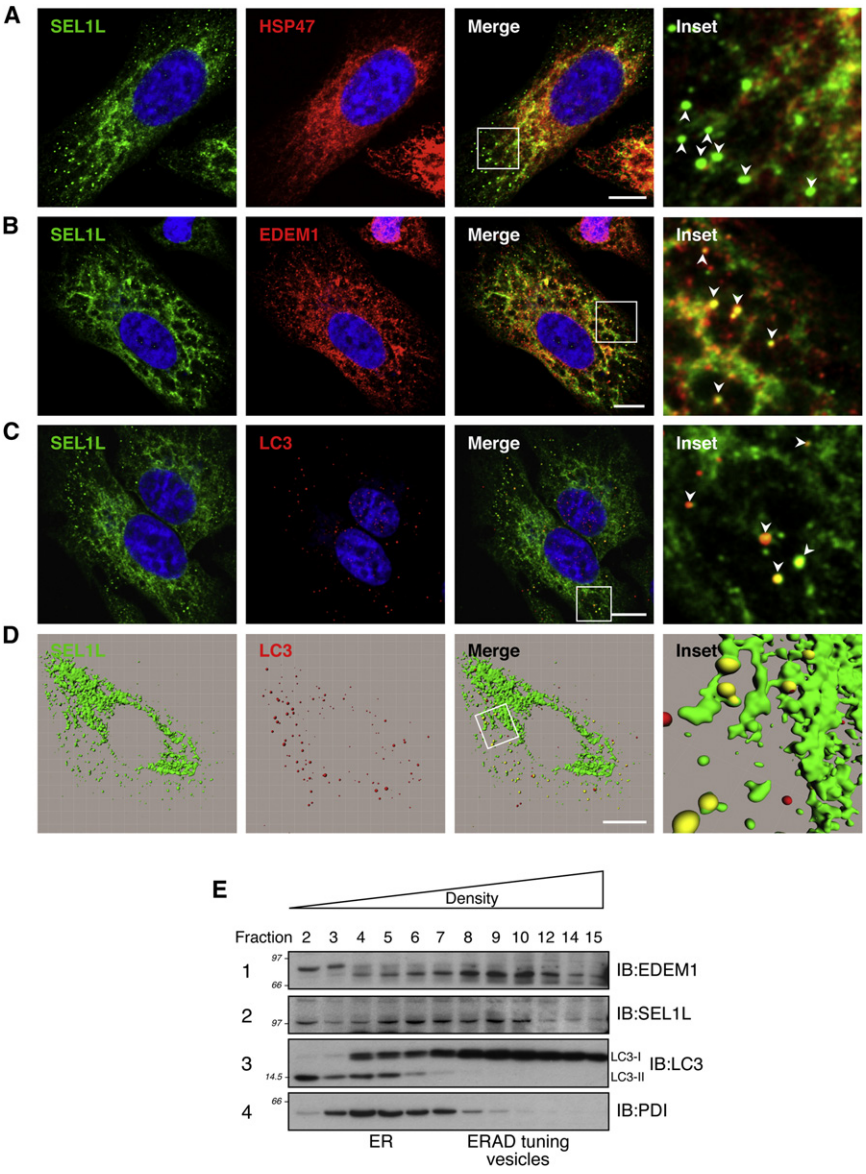

Figure 2. SEL1L in the EDEM1- and in LC3-I-Containing Vesicles

(A–C) Immunofluorescence of CQ-treated HeLa cells. Colocalization of SEL1L with HSP47 (A), EDEM1 (B) or LC3 (C). Arrowheads show SEL1L$^+$/HSP47$^-$, EDEM1$^+$/SEL1L$^+$ or LC3$^+$/SEL1L$^+$ vesicles in (A)–(C), respectively. Scale bar: 10 μm. Additional colocalizations are shown in Figure S3.

(D) Three-dimensional reconstruction of SEL1L:LC3-I colocalization.

(E) Separation of ERAD tuning vesicles from the ER in isopycnic density gradients as thoroughly described in (Calì et al., 2008; Reggiori et al., 2010).

association of LC3-I with SEL1L (Figure 3B, panel 2, lane 3). The coimmunoprecipitation of LC3-I was substantially reduced when the cytosolic tail of SEL1L was replaced with that of CNX (Figure 3B, panel 2, lane 4). In contrast, the presence of LC3-I that was slightly above the background in the CNX immunoisolates (Figure 3B, panel 4, lane 7) was significantly enhanced upon replacement of the cytosolic tail of CNX with that of SEL1L (Figure 3B, panel 4, lane 8). Thus, the cytosolic tail of SEL1L recruits cytosolic LC3-I to the ER-derived vesicles containing EDEM1.

LC3-I Association to the Cytosolic Tail of SEL1L Drives Rerouting to the EDEM1-Containing Vesicles

Next, we assessed the role of the LC3-I-recruiting cytosolic tail of SEL1L in redirecting proteins into the ER-derived vesicles containing EDEM1. To this end, SEL1L (Figure 3C), SEL1L$_{CNX}$ (Figure 3D), CNX (Figure 3E) or CNX$_{SEL1L}$ (Figure 3F) were coexpressed in HeLa cells with LC3-I-HA. The analysis by indirect immunofluorescence confirmed that like the endogenous SEL1L (Figures 2C–2D), a fraction of the ectopically expressed SEL1L colocalized with LC3-I in the ER-derived vesicles (arrowheads in Figure 3C and quantification in Figure 3G). The substitution of the cytosolic tail of SEL1L with the cytosolic tail of CNX resulted in a typical ER staining with the exclusion of the SEL1L$_{CNX}$ chimera from the LC3-I containing structures (Figures 3D and 3G). Like conventional ER chaperones (Figures 2A, 2E, S3D and S4; Calì et al., 2008; Reggiori et al., 2010; Zuber et al., 2007), the ectopically expressed CNX was excluded from the LC3-I positive structures (Figures 3E and 3G). Significantly and consistent with the western blot analysis of the immunocomplexes (Figure 3B), the replacement of the transmembrane and cytosolic domain of CNX with that of SEL1L redirected a fraction of chimeric CNX in the LC3-I-positive ER-derived vesicles (Figures 3F–3G).

Misfolded Proteins Inhibit Formation of ERAD Tuning Vesicles

In cells expressing a folding-defective protein, a lower fraction of endogenous SEL1L is engaged in complexes containing EDEM1 (Figures 1 and S2A) and LC3-I (Figure 4A) and a larger fraction of endogenous SEL1L is engaged in the HRD1 dislocon (Figure S2B). In these cells, the number and the size of the SEL1L/LC3-I-positive vesicles are substantially reduced compared to control cells (Figures 4B–4E). Possibly, SEL1L must be disengaged from the HRD1 dislocon to act as an LC3-I-associated ERAD tuning receptor segregating EDEM1 and OS-9 in the ERAD tuning vesicles. Consistent with this hypothesis, HRD1 is excluded from the ERAD tuning vesicles (Figure S4).

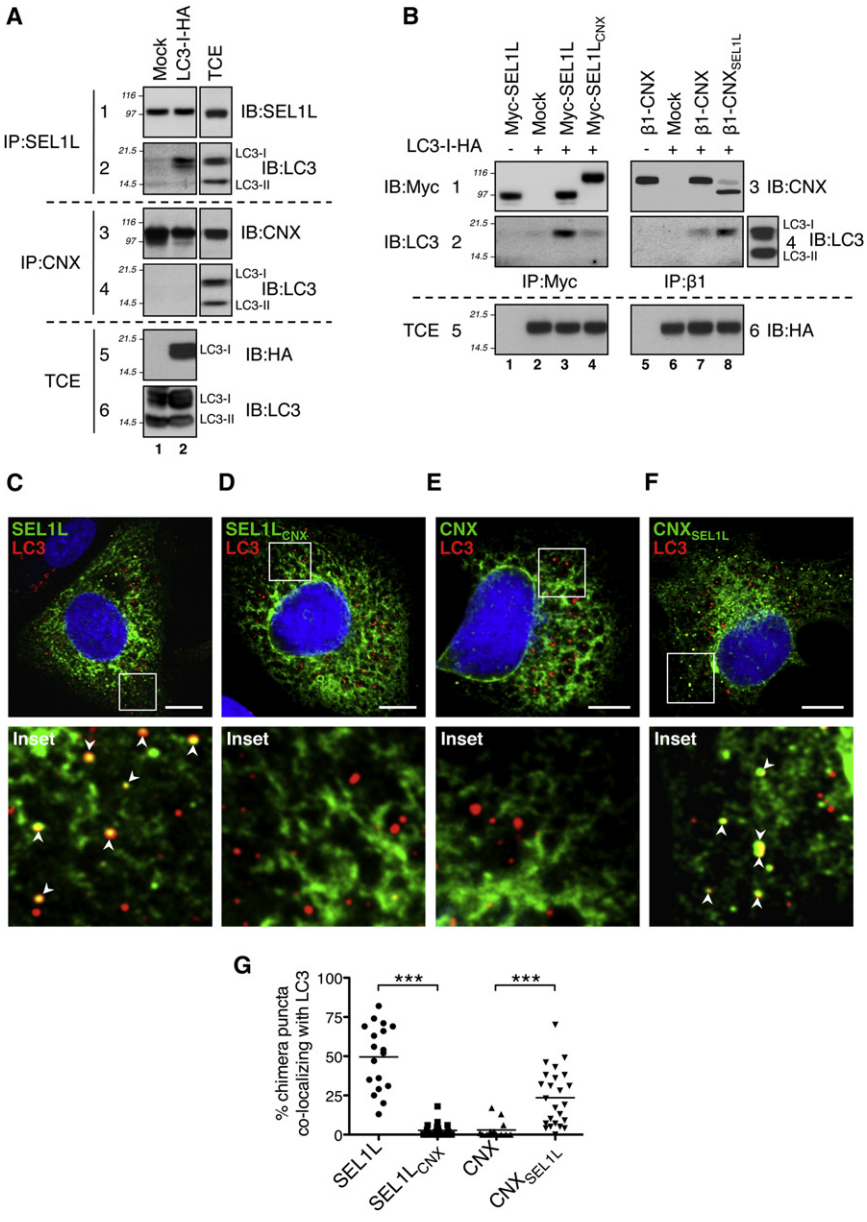

Figure 3. The Cytosolic Tail of SEL1L Binds LC3-I and Drives Segregation into ERAD Tuning Vesicles

(A) Panel 1: Western blot to monitor the level of SEL1L immunoisolated from mock-transfected cells (lane 1) or from cells transfected for expression of LC3-I (lane 2). Panel 2: Level of LC3 in the SEL1L immunocomplexes. Panel 3: Same as panel 1 for CNX. Panel 4: Level of LC3 in the CNX immunocomplexes. Panels 5 and 6: Levels of ectopic LC3-I and total LC3 in the TCE.

(B) Panel 1: Western blot to monitor the level of the Myc-tagged versions of SEL1L (lanes 1 and 3) and SEL1L$_{CNX}$ (lane 4) immunoisolated from cells expressing ectopic LC3-I (lanes 2–4, see panel 5) or from cells not expressing ectopic LC3-I (lane 1). Panel 2: Western blot to monitor, in the same immunoisolates, the presence of LC3-I. Panel 3: Same as Panel 1 for the β1-tagged versions of CNX (lanes 5 and 7) and CNX$_{SEL1L}$ (lane 8). Panel 4: Same as Panel 2 for the immunoisolates containing CNX.

(C) Colocalization of ectopic SEL1L and LC3-I in CQ-treated cells.

(D–F) Same as (C) for SEL1L$_{CNX}$, CNX and CNX$_{SEL1L}$, respectively.

(G) Statistics expressed as the percentage of LC3-I puncta colocalizing with the indicated proteins. Scale bar: 10 μm.

Silencing of SEL1L and of LC3-I Delays Turnover and Increases Intracellular Levels of EDEM1 and OS-9

To gain further evidences on the involvement of SEL1L and LC3-I in ERAD tuning, we assessed the consequences of their silencing on the intracellular level of EDEM1 and OS-9. LC3 silencing (Figure 5A, panel 1, lane 2) increased the endogenous EDEM1 (Figure 5A, panel 3, lane 2) and OS-9 levels (panel 4, lane 2), leaving unaffected the level of the long-living chaperone GRP94 (panel 5 and quantifications). Likewise, SEL1L silencing (Figure 5A, panel 2, lane 3) increased the levels of EDEM1 (Figure 5A, panel 3, lane 3) and OS-9 (Figure 5A, panel 4, lane 3), but not those of GRP94 (panel 5 and quantifications). The inactivation of ERAD tuning by genetic (Calì et al., 2008), pharmacologic and viral interventions (Reggiori et al., 2010) or in cells expressing a folding defective polypeptide (Figures 1 and S2) rises the intracellular levels of EDEM1 and OS-9 by inhibiting their turnover without affecting their synthesis. Likewise, the inactivation of ERAD tuning upon reduction of SEL1L and LC3 expression did not activate UPR programs. This was confirmed by the unchanged intracellular level of GRP94 (Figure 5A, panel 5 and quantifications), by the undetectable levels of transcripts for sXbp1 (Figure 5B) and by the unchanged incorporation of [^{35}S]-methionine/cysteine in nascent endogenous EDEM1 (Figure 5C). Rather, in cells with low content of SEL1L the turnover of EDEM1 (Figure 5D) and OS-9 (Figure 5E, quantifications) were delayed. Altogether, these data are consistent with the identification of SEL1L as the elusive ERAD tuning receptor regulating the selective removal of EDEM1 and OS-9 from the ER (Bernasconi and Molinari, 2011). The lumenal domain of SEL1L selects the cargo proteins entering the ERAD tuning vesicles, the cytosolic tail of SEL1L associates with LC3-I, which drives segregation of the complexes in these ER-derived vesicles. As an additional control, segregation of recombinant EDEM1 into the vesicles, which is normally inefficient possibly because of receptor-saturation (Calì et al., 2008), is enhanced upon coexpression of SEL1L (Figures 5F–5H).

Please cite this article in press as: Bernasconi et al., Role of the SEL1L:LC3-I Complex as an ERAD Tuning Receptor in the Mammalian ER, Molecular Cell (2012), doi:10.1016/j.molcel.2012.04.017

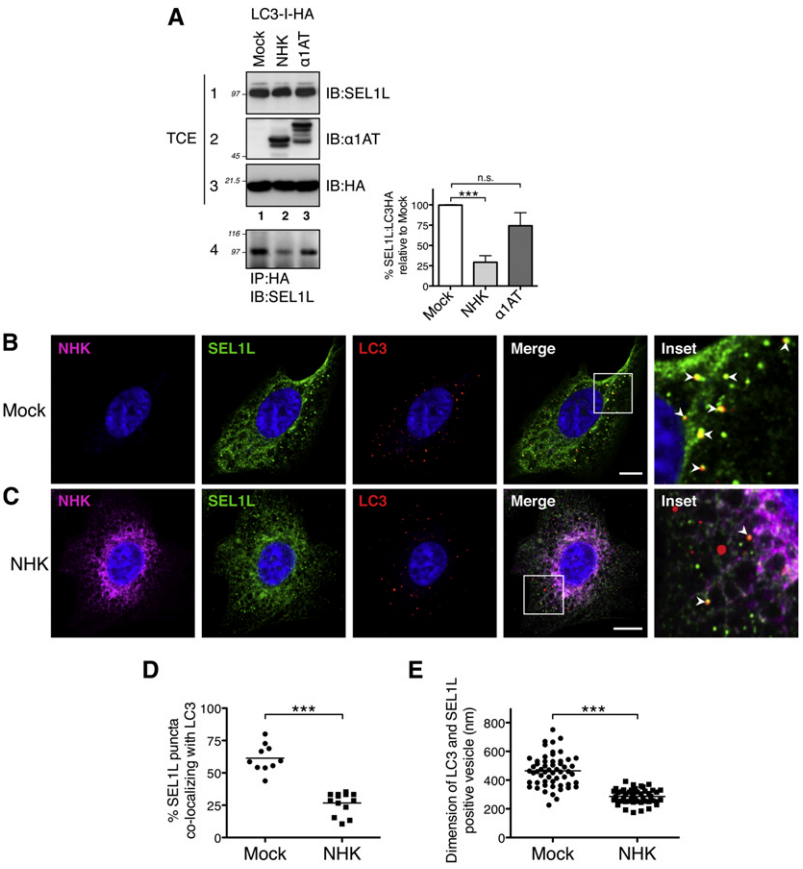

Figure 4. NHK Expression Inhibits Formation of SEL1L:LC3-I Complexes and Reduces Size and Number of ERAD Tuning Vesicles

(A) HeLa cells were transfected for expression of rLC3-I-HA (lane 1), rLC3-I-HA and NHK (lane 2), or rLC3-I-HA and α1AT (lane 3). The levels of endogenous SEL1L (panel 1), NHK and α1AT (panel 2), rLC3-I-HA (panel 3) have been monitored in the total cell lysates (TCE) by western blots. To assess the presence of rLC3-I-HA:SEL1L complexes, rLC3-I-HA was immunoisolated from cell lysates, separated electrophoretically and transferred on PVDF membranes and probed with a SEL1L antiserum (panel 4 and quantification). Error bars: standard deviations from the mean of three replicates.

(B) SEL1L-LC3 colocalization in mock-transfected cells.

(C) Same as (B) in cells expressing the folding-defective NHK-EGFP.

(D and E) Number (D) or size (E) of $SEL1L^{+}/LC3\text{-}I^{+}$ vesicles in cells not expressing or expressing NHK-EGFP.

Inhibition of ERAD Tuning Affects ERAD and Protein Biogenesis

The enhancement of ERAD capacity in cells containing elevated levels of ERAD regulators may compromise the capacity to productively terminate folding programs (e.g., Calì et al. [2008], Tsai et al. [2007], and Wu et al., [2003]). This was confirmed in our experiments where the intracellular content of EDEM1 and OS-9 was increased upon ERAD tuning inactivation resulting from LC3 silencing (Figure 5A). Under these conditions, the disposal of a folding-defective protein was faster as monitored upon quantification of the decay of radiolabeled BACE457Δ (Figures 6A–6B; Molinari et al., 2003). More significantly, the amount of radiolabeled α1AT harvested from the cell culture media was substantially reduced and the fraction of this secretory protein inappropriately selected for disposal increased from less than 5% in control cells to 25%–30% upon ERAD tuning inhibition (Figures 6C–6D). Thus, in a subcellular compartment were folding and selection for disposal of immature polypeptides are in kinetic competition, the regulation of ERAD chaperones turnover by ERAD tuning is crucial to reduce interferences with ongoing folding programs and to maintain cellular proteostasis.

Silencing of SEL1L Inhibits MHV Replication

Infection of mammalian cells with MHV results in the accumulation of putative replication platform vesicles containing viral dsRNA, the host cell proteins LC3-I, EDEM1 and OS-9, but lacking conventional ER markers (de Haan et al., 2010; Reggiori et al., 2010). Consistent with the notion that ERAD tuning vesicles are hijacked during MHV infection, we identified SEL1L as a host protein located in the structures containing viral dsRNA accumulating in MHV infected cells (Figures 6E–6H). Since the downregulation of SEL1L inhibits the vesicle-mediated segregation of EDEM1 and OS-9 from the ER (Figure 5), we hypothesized that MHV replication as well could be impaired. Indeed, silencing of SEL1L caused a 2-fold inhibition of MHV replication as shown by the reduced synthesis of the luciferase reporter gene (Figure 6I), which is stably integrated into the viral genome (de Haan et al., 2005). As previously reported (Reggiori et al., 2010), LC3 silencing inhibited MHV replication, while downregulation of EDEM1 had no effect (Figure 6I) confirming that the receptor complex, but not the cargo of the ERAD tuning vesicles is crucial for efficient viral replication. Altogether, the data shown in Figure 6 support a role of SEL1L as crucial component of the ERAD tuning machinery that sets ERAD activity at levels that do not interfere with protein biogenesis. They also offer additional evidences showing that MHV co-opts ERAD tuning vesicles for replication.

DISCUSSION

ERAD Tuning: the Selective Clearance of ERAD Factors from the ER at Steady State

Molecular chaperones and folding enzymes are long-living proteins. Several regulators of ERAD (e.g., the ERManI [Termine et al., 2009; Wu et al., 2007], HERP [Hori et al., 2004; Miura et al., 2010], SEL1L [Mueller et al., 2006], gp78 [Ballar et al., 2010; Shmueli et al., 2009], EDEM1 and OS-9 [Calì et al., 2008; Le Fourn et al., 2009; Reggiori et al., 2010]) are characterized by faster turnover rates (Figure S1B). Some of them are ubiquitylated and degraded by cytosolic proteasomes (Ballar et al., 2010; Hori et al., 2004; Miura et al., 2010; Mueller et al., 2006; Shmueli et al., 2009). Others, such as EDEM1, OS-9 and the

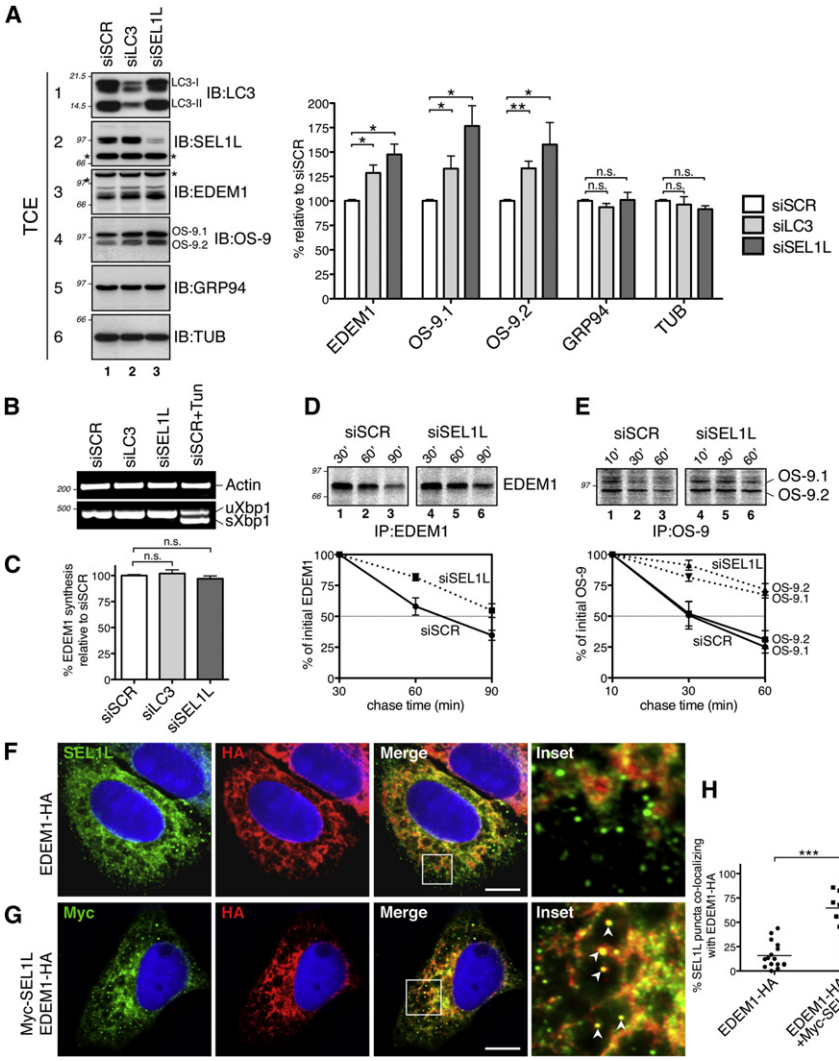

Figure 5. LC3 and SEL1L Silencing Delay the Turnover of Endogenous EDEM1 and OS-9

(A) HeLa cells transfected with a scrambled siRNA (siSCR, lane 1), siLC3 (lane 2) or siSEL1L (lane 3). Levels of LC3, SEL1L, EDEM1, OS-9, GRP94 and Tubulin 2 days later (panels 1–6, respectively). Asterisks are cross-reacting proteins.

(B) Same as Figure 1C.

(C) Quantification of ^{35}S-met/cys incorporation in endogenous EDEM1.

(D) EDEM1 turnover in control cells (siSCR) and in cells with reduced levels of SEL1L (siSEL1L) as determined by immunoprecipitation of the radiolabeled endogenous protein.

(E) Same as (D) for OS-9.1/OS-9.2.

(F and G) HeLa cells were transfected for expression of rEDEM1-HA (F), or rEDEM1-HA and rMyc-SEL1L (G). The cotransfection of SEL1L promotes the segregation of rEDEM1 in the ERAD tuning vesicles.

(H) Statistics expressed as the percentage of SEL1L puncta colocalizing with EDEM1. Scale bars: 10 μm. Error bars: standard deviations from the mean of 3 experimental replicates.

metastasis (Joshi et al., 2010; Tsai et al., 2007), control of hepatitis C virus production (Saeed et al., 2011) and immunoevasion (Tortorella et al., 2000) to name few examples.

The dual Function of SEL1L in Maintenance of Cellular Proteostasis

Cargo proteins are N-glycosylated in the ER lumen. The progressive removal of individual mannose residues signals the ''aging'' of proteins in the folding compartment, i.e., their incapacity to attain the native conformation. The ''rate of aging'' is determined by the intralumenal concentration of mannose processing and mannose-binding proteins such as the ERManI, EDEM1, OS-9, XTP3-B that generate/recognize the protein-bound oligosaccharide code determining the conclusion of the folding-attempts phase and the selection for disposal (Aebi et al., 2010; Molinari, 2007). Enhanced expression (Wu et al., 2003) or defective turnover of these ERAD factors (Calì et al., 2008) may increase the fraction of nascent chains inappropriately destroyed before attainment of the native structure. In addition to recognition of oligosaccharides displayed on folding-defective polypeptides, EDEM1 and OS-9 may use their ML and MRH domains to associate with SEL1L oligosaccharides (Christianson et al., 2012; Christianson et al., 2008; Cormier et al., 2009; Hanna et al., 2012; Satoh et al., 2010). We show that these associations regulate the constitutive, COPII-independent vesicular clearance from the ER of EDEM1, OS-9 and possibly other ERAD regulators such as XTP3-B and EDEM3 (also shown to associate

ERManI are degraded by lysosomal enzymes (Calì et al., 2008; Le Fourn et al., 2009; Reggiori et al., 2010; Wu et al., 2007). The proteasome- and the lysosome-dependent mechanisms regulating the selective clearance of ERAD factors from the ER at steady state are collectively defined as ERAD tuning. ERAD factors should exclusively remove terminally misfolded polypeptides from the ER thereby contrasting their toxic accumulation. If the lumenal concentration of ERAD regulators is aberrantly increased, the resulting enhanced ERAD activity may drastically reduce the time allocated to nascent chains for maturation. Selection of not-yet-native folding intermediates for destruction reduces the overall efficiency of protein biogenesis (e.g., (Calì et al., 2008; Chen et al., 2011; Joshi et al., 2010; Liang et al., 2003; Nunziante et al., 2011; Saeed et al., 2011; Stagg et al., 2009; Tsai et al., 2007; Wang et al., 2012; Wang et al., 2011; Wu et al., 2003; Yamasaki et al., 2005; Younger et al., 2006), this work). Increased intralumenal concentration of ERAD factors might result from increased synthesis or defective turnover and has been linked to loss-of-function phenotypes reported for rheumatoid arthritis (Yamasaki et al., 2005), increased sarcoma

Please cite this article in press as: Bernasconi et al., Role of the SEL1L:LC3-I Complex as an ERAD Tuning Receptor in the Mammalian ER, Molecular Cell (2012), doi:10.1016/j.molcel.2012.04.017

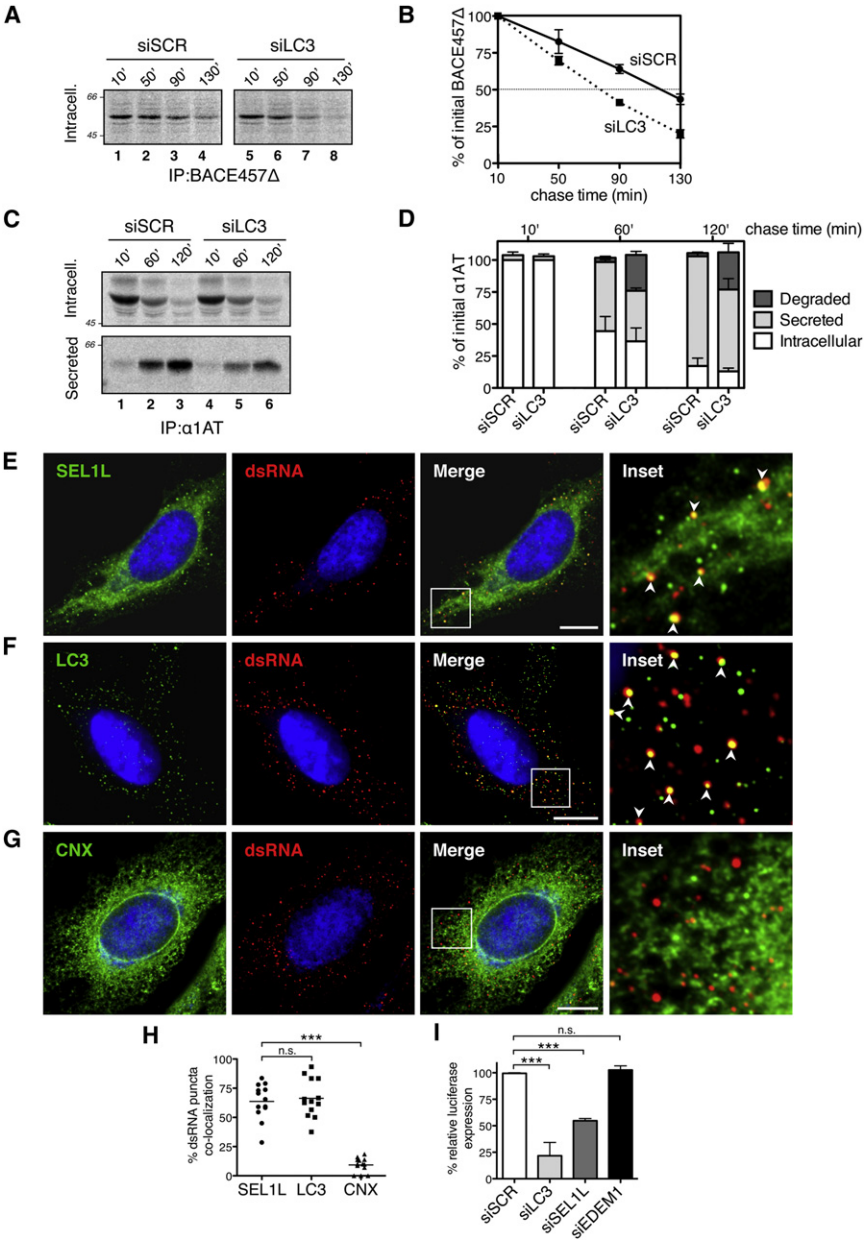

Figure 6. Consequences of ERAD Tuning Inhibition on Protein Quality Control and Viral Replication

(A) Turnover of BACE457Δ in control cells (siSCR) and upon LC3 silencing (siLC3).

(B) Quantification of the decay of the radio-labeled BACE457Δ.

(C) Consequences of LC3 silencing on α1AT biogenesis.

(D) Histogram showing the fraction of α1AT immunoisolated from detergent extracts of cells (intracellular in panel C) or released in the cell culture media (secreted in C) after a 10, 60 and 120 min of chase. The dark gray column shows the fraction of protein degraded.

(E) Colocalization of the endogenous SEL1L with viral dsRNA in cells infected with MHV.

(F) Same as (E) for LC3.

(G) Same as (E) for CNX. Scale bar: 10 μm.

(H) Quantification of (E)–(G).

(I) Quantification of viral replication upon silencing of LC3, SEL1L or EDEM1. Error bars: standard deviations from the mean of 3 experimental replicates.

with SEL1L (Christianson et al., 2012, 2008; Saeed et al., 2011) and the ERManI, which is degraded by lysosomal enzymes (Wu et al., 2007) and is found in EDEM1-containing fractions separated in density gradients (Figure S4). SEL1L plays therefore a dual role in maintenance of cellular proteostasis as an adaptor of the HRD1 dislocation machinery with a well-characterized function in ERAD (Bagola et al., 2011; Hebert et al., 2010) and as part of the membrane-bound receptor regulating the segregation of EDEM1 and OS-9 from the ER lumen. Association of the ubiquitin-like protein LC3-I to the proline-rich cytosolic tail of SEL1L drives the *constitutive* segregation of the EDEM1/OS-9:SEL1L complex into ER-derived vesicles. Folding-defective polypeptides compete with SEL1L for engagement of EDEM1/OS-9 in the ER lumen and also inhibit the association of LC3-I with the cytosolic tail of SEL1L possibly by stabilizing SEL1L in the HRD1 dislocon. It is likely that to act as an ERAD tuning receptor, SEL1L must be disengaged from the dislocation machinery. We postulate that the lumenal absence (Figure 7A) or presence (Figure 7B) of misfolded polypeptides determines the preferential engagement of SEL1L in the ERAD tuning or in the ERAD pathways, respectively.

ERAD Tuning Inhibition by Misfolded Polypeptides

Massive accumulation of folding-defective polypeptides in the ER lumen activates UPR programs resulting in induction of chaperones expression, attenuation of ER cargo load, ER expansion and, eventually, cell death (Walter and Ron, 2011). Our data show that lumenal expression of folding-defective polypeptides at levels that do not induce UPR may selectively enhance ERAD activity by inactivating the ERAD tuning programs (i.e., the constitutive clearance of ERAD factors from the ER) operating at steady state.

Cumulating evidences show that E3 ligases may ubiquitylate themselves (Laney and Hochstrasser, 2002) and other components of the ERAD machinery (e.g., HERP, gp78, SEL1L, ataxin-3) (Ballar et al., 2010; Durcan et al., 2012; Hori et al., 2004; Miura et al., 2010; Mueller et al., 2006; Shmueli et al., 2009) thereby determining their intracellular levels and activities. It is conceivable that also this proteasome-dependent branch of ERAD tuning is inhibited by the lumenal expression of folding-defective polypeptides. These would serve as preferred

Please cite this article in press as: Bernasconi et al., Role of the SEL1L:LC3-I Complex as an ERAD Tuning Receptor in the Mammalian ER, Molecular Cell (2012), doi:10.1016/j.molcel.2012.04.017

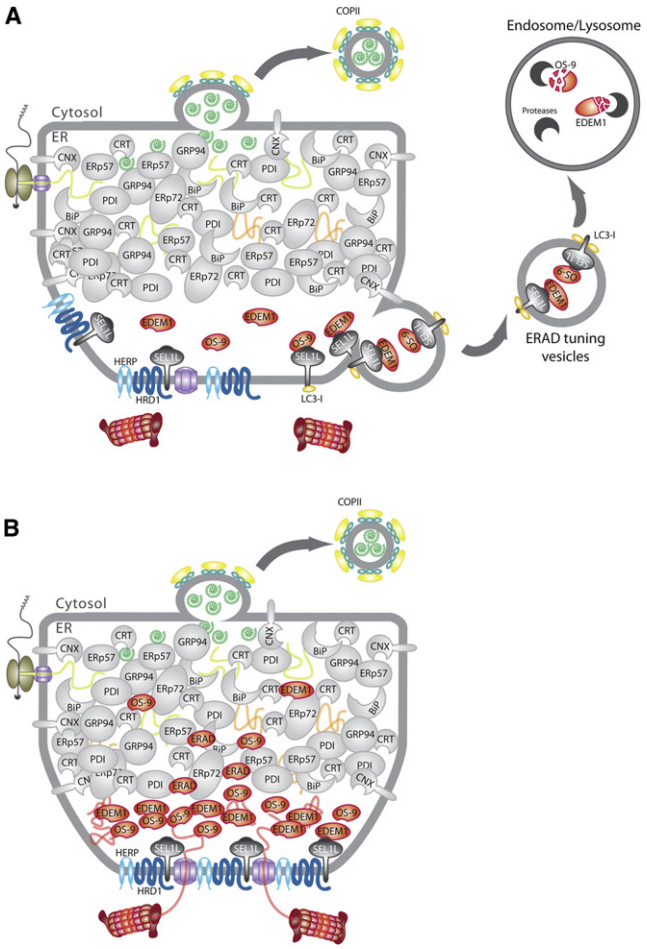

Figure 7. ERAD Tuning: A Model

(A) Steady state situation. ERAD tuning programs lower the concentration of select ERAD factors. The absence of ERAD substrates possibly causes E3 ligase-induced ubiquitylation and degradation of select dislocon proteins (HERP?) with disengagement of the type I protein SEL1L. EDEM1 and OS-9 are segregated in ER-derived ERAD tuning vesicles with intervention of SEL1L and the cytosolic ubiquitin-like protein LC3-I.

(B) Elevation of the intralumenal levels of ERAD substrates inhibits ERAD tuning by stabilizing dislocation machineries and by reducing the interaction of SEL1L with EDEM1, OS-9, and LC3-I. In this situation, the intralumenal concentration of ERAD factors and ERAD activity are enhanced in the absence of UPR-induction.

acceptor for the ubiquitylating activity of the E3 ligases thereby protecting the ERAD machinery from self-destruction (Figure 7B).

All in all, misfolded proteins may enhance the cellular ERAD activity by a sort of autocrine regulatory mechanism(s) that inhibits the constitutive rapid turnover/inactivation of select ERAD factors. This ERAD substrate-induced, UPR-independent enhancement of the ERAD capacity does not require signal transduction from the ER to the nucleus. It therefore represents a more rapid and readily reversible response than UPR-regulated chaperone induction to deal with transient problems that may arise in the folding compartment. In this scenario, UPR induction might eventually occur upon more persistent environmental perturbations or upon substantial lumenal accumulation of folding-defective proteins.

Hijacking of the ERAD Tuning Machinery by CoV

The MHV hijacks components of the ERAD tuning machinery during its infection cycle ((de Haan et al., 2010; Reggiori et al., 2010) and this work). Before our report that this CoV presumably co-opts EDEM1/OS-9/LC3-I-containing vesicles for replication, no host cell protein had been identified in these ER-derived structures that notably lack conventional markers of the secretory pathway. Establishing the role of the ERAD tuning receptor proteins in formation of the ERAD tuning vesicles possibly used as a platform for the replication of the viral genome and the identification of other pathogens that hijack the ERAD tuning machinery for host cell invasion remain matter for future studies.

EXPERIMENTAL PROCEDURES

Expression Plasmids, Antibodies, and Inhibitors

Plasmids encoding ERp27, SEL1L, HRD1 and GFP-LC3 were kind gifts of L. Ruddock, K. Yamamoto, T. Nakajima and N. Mizushima. Plasmids encoding NHK, α1AT (and their membrane-bound variants NHK_B and $\alpha1AT_B$), OS-9 variants, EDEM1, LC3 carrying a G120R mutation, and CNX are described in Bernasconi et al. (2010); Bernasconi et al. (2008); Olivari et al. (2006); and Reggiori et al. (2010). The chimeras $SEL1L_{CNX}$ and CNX_{SEL1L} were generated by fusing the lumenal domain of human SEL1L (1–661) or dog CNX (1–466) with the C-terminal domain of CNX (467–594) or SEL1L (658–791), respectively. Antibodies: Myc and CNX (kind gift of R. Sitia and A. Helenius); HA and α1AT (Sigma); EDEM1 (for IB, Sigma E8406; for IF, Sigma E8159; for IP, Santa Cruz, SC-27391); SEL1L (for IP and IB, Sigma S3699; for IF, kind gift of H.L. Ploegh); HRD1 (for IB, kind gift of T. Nakajima); LC3 (for IB, Sigma L7543; for IF, Nanotool 0231-100), OS-9 (Novus, BC100-520), GRP94 (ABR, MA-3-016). KDEL, PDI, HSP47 (StressGen); dsRNA K1 (English and Scientific Consulting Bt).

Cell Lines, Transient Transfections, and RNA Interferences

HeLa cells were grown in MEM Alpha supplemented with 10% FBS. Cells at 80%–90% confluence were transfected with the expression plasmid of interest using Lipofectamine 2000 (Invitrogen). Experiments were performed 17 hr after transfection. For siRNA-based interference, HeLa cells at 50% confluence in a 3.5 cm tissue culture plate were transfected with siRNA duplex (Ambion Inc, 50 pmol/dish) using Lipofectamine 2000. siRNA targeting sequences: for LC3 (Reggiori et al., 2010); for SEL1L: GGCUAUACUGUGG CUAGAA. Experiments were performed 48 hr after transfection. Stable cell lines have been generated and selected upon transfection of HEK293 cells with an empty plasmid (Mock), a plasmid for expression of a folding defective, membrane-bound variant of NHK (NHK_B), or a plasmid for expression of a membrane-bound variant of secretory protein ($\alpha1AT_B$).

Metabolic Labeling, Immunoprecipitations, Western Blots, Analysis of Data

HeLa cells were pulsed with 0.1 mCi [^{35}S]-methionine/cysteine mix and chased for the indicated times with MEM Alpha supplemented with 5 mM cold methionine and cysteine. Postnuclear supernatant was prepared by solubilization of cells in ice-cold 2% CHAPS (Anatrace) in HEPES-buffered saline (HBS), pH 6.8, containing 20 mM N-ethylmaleimide and protease inhibitors. Immunoprecipitations were performed by adding protein A or G beads (Sigma; 1:10, w/v swollen in HBS) with the selected antibody and incubated for 2 hr to overnight at 4°C. Immunoprecipitates were extensively washed (3x10 min) with 0.5% CHAPS in HBS, resuspended in sample buffer, boiled for 5 min and finally separated in SDS-PAGE. Gels were exposed to BioMax (Kodak) films and scanned with an Agfa scanner. Relevant bands were quantified by

ImageQuant software (Molecular Dynamics). Western blots were performed using the SNAP i.d. system (Millipore). The ECL-Plus detection system was from Amersham, signal was detected using LAS 4000 system and bands were quantified using the Multi Gauge Analysis tool.

Indirect Immunofluorescence Microscopy

HeLa cells were plated 17 hr before fixation on alcian blue-treated glass coverslips. Cells were exposed for 4 hr to 100 μM CQ (to prevent the fusion of EDEM1-containing vesicles with LAMP1-positive degradative organelles) were washed twice with PBS and fixed at RT for 20 min in serum-free buffered medium containing 3.7% formaldehyde. Cells were washed two times with 10 mM HEPES serum-free medium and two times with PBS. The antigen accessibility was improved by a 20 min incubation with 0,05% saponin, 10% Goat serum, 10 mM HEPES and 15 mM glycine (PS). Cells were incubated with the primary antibodies diluted 1:100 in PS for at least 45 min, washed 15 min in PS, then incubated with DAPI (Invitrogen) and Alexa Fluor conjugated secondary antibodies (Invitrogen) diluted 1:200 in PS for at least 30 min. Cells were rinsed with PS and water and mounted in Mowiol. Microscopic images were collected using a laser scanning confocal microscope (Leica DI6000 microscope stand connected to a SP5 scan head) equipped with a HCX PL APO CS 100x1.44 oil UV objective. ImageJ software (version 1.45r) was used for image analysis and processing. The size of the EDEM1/OS-9/LC3-I-containing vesicles has been calculated with the Leica LAS AF software. For the three-dimensional reconstruction, Z stacks were acquired with a step size of 0.13 μm (total size-depth of 4.9 μm). Analysis and reconstruction were prepared using the Imaris x64 software (version 6.1.1; www.bitplane.com).

Semiquantitative Reverse Transcriptase-Polymerase Chain Reactions

HeLa cells were mock-treated or incubated for 12 hr with 2.5 μg/ml tunicamycin. Cells were lyzed in TRIzol reagent (Invitrogen) and RNA was isolated according to the instructions of the manufacturer. Two μg of RNA were used for cDNA synthesis using SuperScriptII reverse transcriptase (Invitrogen) and oligo(dT) (Invitrogen). RT-PCR was performed using *Taq*DNA polymerase (Invitrogen) with transcript-specific primers: unspliced+spliced Xbp1, AAACAGAGTAGCAGCTCAGACTGC (for), TGGCTGGATGAAAGCAG GTT (rev); β-Actin, CTTCCTGGGCATGGAGTCCT (for), GGAGCAATGATCTT GATCTT (rev).

MHV Infection

HeLa cells with a confluency of 50% were inoculated at a moi of 1–10 with recombinant MHV-Srec expressing the firefly luciferase gene (de Haan et al., 2005) for 1 hr at 37°C. The viral media was then replaced with fresh medium and cells were incubated for 6 hr at 37°C. Virus replication was quantified by measuring the luciferase expression using the firefly luciferase assay kit (Steadylite plus, PerkinElmer) according to the manufacturer's instructions. Alternatively, cells were fixed in 4% PFA and analyzed by confocal microscopy.

Statistical Analysis

At least three independent experiments were quantified, analyzed with the Prism 5 software and plotted as the mean ± standard deviation. Unpaired student's t test was used to compare the mean of control and experimental groups. The p value was defined as follow: not significant (n.s.): $p > 0.05$; *: $p < 0.05$; **: $p < 0.01$; ***: $p < 0.001$. All p values are two tailed.

SUPPLEMENTAL INFORMATION

Supplemental Information includes five figures and can be found with this article online at doi:10.1016/j.molcel.2012.04.017.

ACKNOWLEDGMENTS

We would like to thank M. Aebi, E. Fasana, R. Gauss, A. Helenius, D. Hebert, L. Ruddock, and R. Sitia for insightful comments and discussions; L. Ruddock, K. Yamamoto, N. Mizushima, T. Nakajima, H.L. Ploegh, and S. Tolchinsky for providing various reagents; Iryna Monastyrska, M. Thelen, and E. Montani for the assistance during microscope imaging, and M. Hunziker. M.M. is supported by grants from the Foundation for Research on Neurodegenerative Diseases, the Fondazione San Salvatore, the Swiss National Science Foundation, the Association Française contre les Myopathies, the Novartis Stiftung für medizinisch-biologische Forschung and the Gabriele Foundation. C.A.M.d.H. was supported by a grant from the Netherlands Organization for Scientific Research (NWO-ALW). F.R. is supported by the Netherlands Organization for Scientific Research (Chemical Sciences, ECHO grant-700.59.003; Earth and Life Sciences, Open Program grant-821.02.017; Cooperation Germany-DN82-303).

Received: March 23, 2011
Revised: September 1, 2011
Accepted: April 12, 2012
Published online: May 24, 2012

REFERENCES

Aebi, M., Bernasconi, R., Clerc, S., and Molinari, M. (2010). N-glycan structures: recognition and processing in the ER. Trends Biochem. Sci. *35*, 74–82.

Bagola, K., Mehnert, M., Jarosch, E., and Sommer, T. (2011). Protein dislocation from the ER. Biochim. Biophys. Acta *1808*, 925–936.

Ballar, P., Ors, A.U., Yang, H., and Fang, S. (2010). Differential regulation of CFTRDeltaF508 degradation by ubiquitin ligases gp78 and Hrd1. Int. J. Biochem. Cell Biol. *42*, 167–173.

Bernasconi, R., and Molinari, M. (2011). ERAD and ERAD tuning: disposal of cargo and of ERAD regulators from the mammalian ER. Curr. Opin. Cell Biol. *23*, 176–183.

Bernasconi, R., Pertel, T., Luban, J., and Molinari, M. (2008). A dual task for the Xbp1-responsive OS-9 variants in the mammalian endoplasmic reticulum: inhibiting secretion of misfolded protein conformers and enhancing their disposal. J. Biol. Chem. *283*, 16446–16454.

Bernasconi, R., Galli, C., Calanca, V., Nakajima, T., and Molinari, M. (2010). Stringent requirement for HRD1, SEL1L, and OS-9/XTP3-B for disposal of ERAD-LS substrates. J. Cell Biol. *188*, 223–235.

Calì, T., Galli, C., Olivari, S., and Molinari, M. (2008). Segregation and rapid turnover of EDEM1 by an autophagy-like mechanism modulates standard ERAD and folding activities. Biochem. Biophys. Res. Commun. *371*, 405–410.

Chen, X., Tukachinsky, H., Huang, C.H., Jao, C., Chu, Y.R., Tang, H.Y., Mueller, B., Schulman, S., Rapoport, T.A., and Salic, A. (2011). Processing and turnover of the Hedgehog protein in the endoplasmic reticulum. J. Cell Biol. *192*, 825–838.

Christianson, J.C., Shaler, T.A., Tyler, R.E., and Kopito, R.R. (2008). OS-9 and GRP94 deliver mutant alpha1-antitrypsin to the Hrd1-SEL1L ubiquitin ligase complex for ERAD. Nat. Cell Biol. *10*, 272–282.

Christianson, J.C., Olzmann, J.A., Shaler, T.A., Sowa, M.E., Bennett, E.J., Richter, C.M., Tyler, R.E., Greenblatt, E.J., Harper, J.W., and Kopito, R.R. (2012). Defining human ERAD networks through an integrative mapping strategy. Nat. Cell Biol. *14*, 93–105.

Cormier, J.H., Tamura, T., Sunryd, J.C., and Hebert, D.N. (2009). EDEM1 recognition and delivery of misfolded proteins to the SEL1L-containing ERAD complex. Mol. Cell *34*, 627–633.

de Haan, C.A., Li, Z., te Lintelo, E., Bosch, B.J., Haijema, B.J., and Rottier, P.J. (2005). Murine coronavirus with an extended host range uses heparan sulfate as an entry receptor. J. Virol. *79*, 14451–14456.

de Haan, C.A., Molinari, M., and Reggiori, F. (2010). Autophagy-independent LC3 function in vesicular traffic. Autophagy *6*, 994–996.

Durcan, T.M., Kontogiannea, M., Bedard, N., Wing, S.S., and Fon, E.A. (2012). Ataxin-3 deubiquitination is coupled to Parkin ubiquitination via E2 ubiquitin-conjugating enzyme. J. Biol. Chem. *287*, 531–541.

Hanna, J., Schütz, A., Zimmermann, F., Behlke, J., Sommer, T., and Heinemann, U. (2012). Structural and biochemical basis of Yos9 protein

dimerization and possible contribution to self-association of 3-hydroxy-3-methylglutaryl-coenzyme A reductase degradation ubiquitin-ligase complex. J. Biol. Chem. *287*, 8633–8640.

Hebert, D.N., Bernasconi, R., and Molinari, M. (2010). ERAD substrates: which way out? Semin. Cell Dev. Biol. *21*, 526–532.

Helenius, A. (1994). How N-linked oligosaccharides affect glycoprotein folding in the endoplasmic reticulum. Mol. Biol. Cell *5*, 253–265.

Hori, O., Ichinoda, F., Yamaguchi, A., Tamatani, T., Taniguchi, M., Koyama, Y., Katayama, T., Tohyama, M., Stern, D.M., Ozawa, K., et al. (2004). Role of Herp in the endoplasmic reticulum stress response. Genes Cells *9*, 457–469.

Joshi, B., Li, L., and Nabi, I.R. (2010). A role for KAI1 in promotion of cell proliferation and mammary gland hyperplasia by the gp78 ubiquitin ligase. J. Biol. Chem. *285*, 8830–8839.

Kabeya, Y., Mizushima, N., Ueno, T., Yamamoto, A., Kirisako, T., Noda, T., Kominami, E., Ohsumi, Y., and Yoshimori, T. (2000). LC3, a mammalian homologue of yeast Apg8p, is localized in autophagosome membranes after processing. EMBO J. *19*, 5720–5728.

Laney, J.D., and Hochstrasser, M. (2002). Analysis of protein ubiquitination. Curr. Protoc. Protein Sci., *Chapter 14*, 14, 5.

Le Fourn, V., Gaplovska-Kysela, K., Guhl, B., Santimaria, R., Zuber, C., and Roth, J. (2009). Basal autophagy is involved in the degradation of the ERAD component EDEM1. Cell. Mol. Life Sci. *66*, 1434–1445.

Lederkremer, G.Z. (2009). Glycoprotein folding, quality control and ER-associated degradation. Curr. Opin. Struct. Biol. *19*, 515–523.

Liang, J.S., Kim, T., Fang, S., Yamaguchi, J., Weissman, A.M., Fisher, E.A., and Ginsberg, H.N. (2003). Overexpression of the tumor autocrine motility factor receptor Gp78, a ubiquitin protein ligase, results in increased ubiquitinylation and decreased secretion of apolipoprotein B100 in HepG2 cells. J. Biol. Chem. *278*, 23984–23988.

Miura, H., Hashida, K., Sudo, H., Awa, Y., Takarada-Iemata, M., Kokame, K., Takahashi, T., Matsumoto, M., Kitao, Y., and Hori, O. (2010). Deletion of Herp facilitates degradation of cytosolic proteins. Genes Cells *15*, 843–853.

Molinari, M. (2007). N-glycan structure dictates extension of protein folding or onset of disposal. Nat. Chem. Biol. *3*, 313–320.

Molinari, M., Calanca, V., Galli, C., Lucca, P., and Paganetti, P. (2003). Role of EDEM in the release of misfolded glycoproteins from the calnexin cycle. Science *299*, 1397–1400.

Mueller, B., Lilley, B.N., and Ploegh, H.L. (2006). SEL1L, the homologue of yeast Hrd3p, is involved in protein dislocation from the mammalian ER. J. Cell Biol. *175*, 261–270.

Nunziante, M., Ackermann, K., Dietrich, K., Wolf, H., Gädtke, L., Gilch, S., Vorberg, I., Groschup, M., and Schätzl, H.M. (2011). Proteasomal dysfunction and endoplasmic reticulum stress enhance trafficking of prion protein aggregates through the secretory pathway and increase accumulation of pathologic prion protein. J. Biol. Chem. *286*, 33942–33953.

Olivari, S., Cali, T., Salo, K.E., Paganetti, P., Ruddock, L.W., and Molinari, M. (2006). EDEM1 regulates ER-associated degradation by accelerating de-mannosylation of folding-defective polypeptides and by inhibiting their covalent aggregation. Biochem. Biophys. Res. Commun. *349*, 1278–1284.

Reggiori, F., Monastyrska, I., Verheije, M.H., Calì, T., Ulasli, M., Bianchi, S., Bernasconi, R., de Haan, C.A., and Molinari, M. (2010). Coronaviruses Hijack the LC3-I-positive EDEMosomes, ER-derived vesicles exporting short-lived ERAD regulators, for replication. Cell Host Microbe *7*, 500–508.

Saeed, M., Suzuki, R., Watanabe, N., Masaki, T., Tomonaga, M., Muhammad, A., Kato, T., Matsuura, Y., Watanabe, H., Wakita, T., and Suzuki, T. (2011). Role of the endoplasmic reticulum-associated degradation (ERAD) pathway in degradation of hepatitis C virus envelope proteins and production of virus particles. J. Biol. Chem. *286*, 37264–37273.

Satoh, T., Chen, Y., Hu, D., Hanashima, S., Yamamoto, K., and Yamaguchi, Y. (2010). Structural basis for oligosaccharide recognition of misfolded glycoproteins by OS-9 in ER-associated degradation. Mol. Cell *40*, 905–916.

Shmueli, A., Tsai, Y.C., Yang, M., Braun, M.A., and Weissman, A.M. (2009). Targeting of gp78 for ubiquitin-mediated proteasomal degradation by Hrd1: cross-talk between E3s in the endoplasmic reticulum. Biochem. Biophys. Res. Commun. *390*, 758–762.

Smith, M.H., Ploegh, H.L., and Weissman, J.S. (2011). Road to ruin: targeting proteins for degradation in the endoplasmic reticulum. Science *334*, 1086–1090.

Stagg, H.R., Thomas, M., van den Boomen, D., Wiertz, E.J., Drabkin, H.A., Gemmill, R.M., and Lehner, P.J. (2009). The TRC8 E3 ligase ubiquitinates MHC class I molecules before dislocation from the ER. J. Cell Biol. *186*, 685–692.

Tamura, T., Sunryd, J.C., and Hebert, D.N. (2010). Sorting things out through endoplasmic reticulum quality control. Mol. Membr. Biol. *27*, 412–427.

Termine, D.J., Moremen, K.W., and Sifers, R.N. (2009). The mammalian UPR boosts glycoprotein ERAD by suppressing the proteolytic downregulation of ER mannosidase I. J. Cell Sci. *122*, 976–984.

Tortorella, D., Gewurz, B.E., Furman, M.H., Schust, D.J., and Ploegh, H.L. (2000). Viral subversion of the immune system. Annu. Rev. Immunol. *18*, 861–926.

Tsai, Y.C., Mendoza, A., Mariano, J.M., Zhou, M., Kostova, Z., Chen, B., Veenstra, T., Hewitt, S.M., Helman, L.J., Khanna, C., and Weissman, A.M. (2007). The ubiquitin ligase gp78 promotes sarcoma metastasis by targeting KAI1 for degradation. Nat. Med. *13*, 1504–1509.

Vembar, S.S., and Brodsky, J.L. (2008). One step at a time: endoplasmic reticulum-associated degradation. Nat. Rev. Mol. Cell Biol. *9*, 944–957.

Walter, P., and Ron, D. (2011). The unfolded protein response: from stress pathway to homeostatic regulation. Science *334*, 1081–1086.

Wang, F., Song, W., Brancati, G., and Segatori, L. (2011). Inhibition of endoplasmic reticulum-associated degradation rescues native folding in loss of function protein misfolding diseases. J. Biol. Chem. *286*, 43454–43464.

Wang, F., Olson, E.M., and Shyng, S.-L. (2012). Role of Derlin-1 in Proteostasis Regulation of ATP-sensitive Potassium Channels. J Biol Chem. *287*, 10482–10493.

Wu, Y., Swulius, M.T., Moremen, K.W., and Sifers, R.N. (2003). Elucidation of the molecular logic by which misfolded alpha 1-antitrypsin is preferentially selected for degradation. Proc. Natl. Acad. Sci. USA *100*, 8229–8234.

Wu, Y., Termine, D.J., Swulius, M.T., Moremen, K.W., and Sifers, R.N. (2007). Human endoplasmic reticulum mannosidase I is subject to regulated proteolysis. J. Biol. Chem. *282*, 4841–4849.

Yamasaki, S., Yagishita, N., Tsuchimochi, K., Nishioka, K., and Nakajima, T. (2005). Rheumatoid arthritis as a hyper-endoplasmic-reticulum-associated degradation disease. Arthritis Res. Ther. *7*, 181–186.

Younger, J.M., Chen, L., Ren, H.Y., Rosser, M.F., Turnbull, E.L., Fan, C.Y., Patterson, C., and Cyr, D.M. (2006). Sequential quality-control checkpoints triage misfolded cystic fibrosis transmembrane conductance regulator. Cell *126*, 571–582.

Zuber, C., Cormier, J.H., Guhl, B., Santimaria, R., Hebert, D.N., and Roth, J. (2007). EDEM1 reveals a quality control vesicular transport pathway out of the endoplasmic reticulum not involving the COPII exit sites. Proc. Natl. Acad. Sci. USA *104*, 4407–4412.